ISSN 0016-7932, Geomagnetism and Aeronomy, 2011, Vol. 51, No. 1, pp. 49–65. © Pleiades Publishing, Ltd., 2011.
Original Russian Text © N.S. Nikolaeva, Yu.I. Yermolaev, I.G. Lodkina, 2011, published in Geomagnetizm i Aeronomiya, 2011, Vol. 51, No. 1, pp. 51–67.

Dependence of Geomagnetic Activity during Magnetic Storms on the Solar Wind Parameters for Different Types of Streams

N. S. Nikolaeva, Yu. I. Yermolaev, and I. G. Lodkina

Space Research Institute, Russian Academy of Sciences, Profsoyuznaya ul. 84/32, Moscow, 117997 Russia
e-mail: nnikolae@iki.rssi.ru

Received December 10, 2009; in final form, August 10, 2010

Abstract—The dependence of the maximal values of the $|Dst|$ and AE geomagnetic indices observed during magnetic storms on the value of the interplanetary electric field (E_y) was studied based on the catalog of the large-scale solar wind types created using the OMNI database for 1976–2000 [Yermolaev et al., 2009]. An analysis was performed for eight categories of magnetic storms caused by different types of solar wind streams: corotating interaction regions (CIR, 86 storms); magnetic clouds (MC, 43); Sheath before MCs (Sh_{MC}, 8); Ejecta (95); Sheath (Sh_E, 56); all ICME events (MC + Ejecta, 138); all compression regions Sheaths before MCs and Ejecta ($Sh_{MC} + Sh_E$, 64); and an indeterminate type of storm (IND, 75). It was shown that the $|Dst|$ index value increases with increasing electric field E_y for all eight types of streams. When electric fields are strong ($E_y > 11$ mV m^{-1}), the $|Dst|$ index value becomes saturated within magnetic clouds MCs and possibly within all ICMEs (MC + Ejecta). The AE index value during magnetic storms is independent of the electric field value E_y for almost all streams except magnetic clouds MCs and possibly the compressed (Sheath) region before them (Sh_{MC}). The AE index linearly increases within MC at small values of the electric field ($E_y <$ 11 mV m^{-1}) and decrease when these fields are strong ($E_y > 11$ mV m^{-1}). Since the dynamic pressure (Pd) and IMF fluctuations (σB) correlate with the E_y value in all solar wind types, both geomagnetic indices ($|Dst|$ and AE) do not show an additional dependence on Pd and IMF σB. The nonlinear relationship between the intensities of the $|Dst|$ and AE indices and the electric field E_y component, observed within MCs and possibly all ICMEs during strong electric fields E_y, agrees with modeling the magnetospheric–ionospheric current system of zone 1 under the conditions of the polar cap potential saturation.

DOI: 10.1134/S0016793211010099

1. INTRODUCTION

Numerous experiments have indicated that magnetic storms are mainly caused by southward IMF (see, e.g., [Russell et al., 1974; Burton et al., 1975; Akasofu et al., 1985; Gonzalez et al., 1999; O'Brien and McPherron, 2000; Vennerstroem, 2001; Yermolaev and Yermolaev, 2002; Sheath Lyatsky and Tan, 2003; Huttunen and Koskinen, 2004; Rusanov and Petrukovich, 2004; Maltsev, 2004; Veselovsky et al., 2004; Gonzalez and Echer, 2005; Yermolaev et al., 2005a, 2005b, 2007a] and references therein). The effectiveness of the IMF B_z component in the generation of magnetic storms and substorms depends on the interaction between the induced electric field $E_y = V_x B_z$ (V_x is the radial component of the solar wind velocity at the southward IMF component $B_z < 0$) and the magnetospheric–ionospheric system. The distribution of currents within this system changes as a result of these processes (see, e.g., [Gonzalez et al., 1994; O'Brien and McPherron, 2000; Siscoe et al., 2005; Zhu et al., 2006] and references therein), which affects the magnetic field value on the Earth's surface and leads to changes in the value of the geomagnetic indices.

The intensity of a magnetospheric disturbance is estimated using the Dst and AE indices. The high-latitude AE index characterizes the intensity of the auroral electrojet current and is the indicator of substorm activity [Davis and Sugiura, 1966]. The low-latitude Dst index is used to estimate the ring current intensity during magnetic storms and is the measure of the interplanetary disturbance geoeffectiveness [Sugiura, 1964; Burton et al., 1975]. We emphasize that auroral activity during magnetic storms has been studied. Substorms without magnetic storms possibly develop differently: e.g., Alfvén waves can cause substorms but cannot cause storms (see [McPherron et al., 2009] and references therein). In addition, during magnetic storms auroral electrojets shift to lower latitudes relative to the latitude of the stations used to determine the AE index, and results can be distorted [Feldstein, 1992].

The electric field E_y is the main solar wind parameter for the generation of magnetic storms and substorms. At the same time, the magnetic storm intensity

is also affected by variations in other solar wind parameters: dynamic pressure *Pd* and IMF σB fluctuations [Burton et al., 1975; Gonzalez et al., 2001, 2002; Borovsky and Funstein, 2003; Seki et al., 2005; Yermolaev et al., 2007a, 2007b]. The relative contribution of the dynamic pressure *Pd* to the *Dst* index value is not a constant value as followed from the work (see [Burton et al., 1975]). The effect of *Pd* on the *Dst* index value depends on the value of the electric field component E_y and the contribution of *Pd* is insignificant at the large E_y values usually observed during the main storm phases [Siscoe et al., 2002, 2005].

An ordinary quasistationary solar wind does not contain a considerable and prolonged IMF B_z component sufficient for the generation of a magnetic storm. At the same time, certain disturbed types of solar wind streams can have a large and prolonged IMF B_z component, including such a component oriented southward, which results in a magnetic storm [Tsurutani et al., 1988, 1995; Yermolaev and Yermolaev, 2002; Huttunen and Koskinen, 2004; Huttunen et al., 2002; Richardson et al., 2002; Vieira et al., 2004; Echer and Gonzalez, 2004; Yermolaev et al., 2005a, 2010a].

Several geoeffective solar wind streams, during the passage of which magnetic storms with different intensities are observed, can be distinguished. Interplanetary manifestations of coronal mass ejections CMEs (ICME events including two subtypes: magnetic clouds MCs and Ejecta) and the regions where high-speed solar wind streams interact with slow streams (CIRs) are the main types of these streams. The studies indicated that the region of compressed plasma (Sheath) can be observed before the ICME forward front (before MC, Sh_{MC} or Ejecta "piston", Sh_E). The nature of the Sheath formation is close to that of CIRs; however, ICME plays the role of a "piston" in this case instead of a high-speed solar wind stream. Each stream type has its own set of solar wind parameters different from other stream types. For example, at the front of high- and low-speed streams in (CIR events) and before the "piston" forward front (Sheath), plasma has increased values of density and temperature, and the thermal pressure predominates over the magnetic one $\beta > 1$. A magnetic cloud is a subclass of ICME events and has a higher (>10 nT) and more regular magnetic field than Ejecta. Both subtypes of ICME events (MC + Ejecta) have a magnetic field structure in the form of a rope and the magnetic pressure predominates over the thermal one within them ($\beta \ll 1$). Note that we do not consider the class of very strong magnetic storms that are generated by several ICMEs interacting with one another [Yermolaev and Yermolaev, 2008]. The method for identifying different types of solar wind streams based on the OMNI plasma and magnetic database for 1976–2000 is described in detail in [Yermolaev et al., 2009]. The complete statistics of the solar wind events are presented and their geoeffectiveness as the magnetic storm occurrence probability (i.e., the ratio of the number of events that caused a magnetic storm to the total number of events of a given type) is estimated in [Yermolaev et al., 2010a]. It is known that the development of geomagnetic storms and substorms substantially differs depending on the stream type that caused these phenomena [Borovsky and Denton, 2006; Despirak et al., 2009]. In particular, these differences are observed in the behavior of the ring current, aurora, and Earth's plasma sheet; in magnetospheric convection; and in the polar cap potential saturation [Borovsky and Denton, 2006].

The works devoted to the relationship between the *Dst* index minimum and the IMF B_z component mostly ignore the types of interplanetary disturbances that generated magnetic storms (see, e.g., [Akasofu et al., 1985; O'Brien and McPherron, 2000] and references therein). The situation is similar concerning the dependence of the *AE* index on E_y (see, e.g., [Weimer et al., 1990]). Only some works have considered the relationship between these parameters in specific types of solar wind streams: MCs [Wu and Lepping, 2002; Yurchyshyn et al., 2004; Yermolaev et al., 2007b], corotating interaction regions CIR [Alves et al., 2006; Richardson et al., 2006; Yermolaev et al., 2007b], or streams behind interplanetary shocks [Oh and Yi, 2004].

The number of the works comparing these dependences in different stream types with different internal structures is even smaller. The characteristics of the electric field E_y variations during the passage of two main solar wind types (MCs and CIRs) were compared in [Kershendolts et al., 2007; Plotnikov and Barkova, 2007]. The authors indicated that a nonlinear dependence of the *AE* and $|Dst|$ indices on E_y is observed for MCs. These indices linearly increase with increasing electric field at small values ($E_y < 12$ mV m^{-1}). When the field is large ($E_y > 12$ mV m^{-1}), the $|Dst|$ index becomes saturated, and the *AE* index decreases [Kershendolts et al., 2007; Plotnikov and Barkova, 2007]. At the same time, both indices linearly vary in the entire E_y range for CIR. The authors also studied the relationship of the indices with the dynamic pressure and IMF fluctuation level observed in MC and CIR. In this case the maximal hourly values of the $|Dst|$ and *AE* indices within MC and CIR were compared with the *Pd* value and IMF fluctuation level in Sheath before MC. The authors found that the relationships between the indices and solar wind parameters are significant for CIR ($r > 0.5$) and are insignificant for MC ($r < 0.5$). The internal structure of MCs themselves and their possible division into two parts (the Sheath before MC and the MC body) was factually ignored in these works [Kershendolts et al., 2007; Plotnikov and Barkova, 2007] when the dependences of the indices on E_y were studied.

In our previous work [Yermolaev et al., 2007b], we considered the region of ICME itself (i.e., the sum of

MC and Ejecta) and the Sheath before them (Sh_{MC} + Sh_E) as two different types of solar wind streams. This work [Yermolaev et al., 2007b] compared the dependences of the *Dst* index minimum on the electric field E_y component for four types of the solar wind events: ICMEs (MC + Ejecta), corotating solar wind streams CIRs, Sheath (Sh_{MC} + Sh_E), and events of an indeterminate type. In addition, the achieved results were also compared with the data obtained by other authors [Wu and Lepping, 2002, 2005; Alves et al., 2006; Srivastava and Venkatakrishnan, 2004; Kane, 2005]. However, in [Yermolaev et al., 2007b] we used only linear dependences for regression lines and did not numerically estimate the correlation ratio (correlation coefficients).

The present work continues the previous one [Yermolaev et al., 2007b], but we decreased the *Dst* threshold at a storm minimum from −60 to −50 nT in order to increase the magnetic storm statistics; i.e., all moderate magnetic storms were analyzed. Second, we divided all moderate magnetic storms into eight groups (instead of four groups) depending on the type of a solar wind stream that caused a magnetic storm. The main aim of this work is to study the correlations between the magnetic storm intensities (the *Dst* index minimum and the |*Dst*| value are used) and substorm activity (the *AE* index) during a storm and the main solar wind parameters: the E_y component of the solar wind electric field, dynamic pressure *Pd*, and IMF fluctuation level σB. We analyze the values of the geomagnetic indices and solar wind parameters observed at a peak of the magnetic storm main phase. The main novelty of our paper consists in that we compare the response of the magnetosphere to different interplanetary drivers, the list of which is presented most completely at the modern stage of science. This approach should be first tested using the simplest method for comparing interplanetary and magnetospheric conditions and then developed based on more physically perfect concepts (we have continued working in this field and published certain data on studying the dynamics of development of geomagnetic indices and solar wind parameters during the entire main phase of magnetic storms [Yermolaev et al., 2010b]). Our method for characterizing storms using the minimal negative value of the *Dst* index is one of the simplified methods used to compare magnetic storms and their geoeffectiveness with the solar wind. For example, it is better to characterize the complete magnetic storm intensity by comparing the total geomagnetic index for the storm period with the solar wind electric field during the storm period or with the Akasofu parameter; however, this subject is outside the scope of this study. According to our method of analysis, it is implicitly assumed that the time of the magnetospheric response to the solar wind is not more than 1 h. At the same time, studying the dynamics of development of the geomagnetic indices and solar wind parameters during the entire magnetic storm main phase indicates that a magnetic storm "remembers" previous B_z (and E_y) values [Yermolaev et al., 2010b]. Geomagnetic indices can theoretically correlate with many solar wind parameters; however, the number of independent parameters affecting indices can be small since these parameters are interrelated. The number of these parameters and what parameters should be used is the problem to be solved in the present study.

2. METHOD

The list of magnetic storms with the minimum of $Dst \le -50$ nT during the 1976–2000 period, for which the source was found in the solar wind [Yermolaev et al., 2009] was used as initial data for studying the interrelation between the *Dst* and *AE* geomagnetic indices, the solar wind parameters (the electric field E_y component and dynamic pressure *Pd*), and the IMF σB fluctuation level. The method for identifying different types of the solar wind stream related to magnetic storms were described in detail in [Yermolaev et al., 2009, 2010a]. The list of magnetic storms with $Dst \le -50$ nT was completed with the data on the following quantities: the dynamic pressure *Pd*, IMF σB fluctuation level, and *AE* index at a minimum of the magnetic storm *Dst* index (i.e., we used the *AE* index value at the instant when *Dst* was minimal averaged over 1 h rather than the maximal *AE* value). The *AE* index values averaged over 1 h were taken from the OMNI 2 database (http://omniweb.gsfc.nasa.gov/form/dx1.html) [King and Papitashvili, 2004]. In addition, we estimated the E_y component of the convective electric field ($E_y = V_x B_z$, where V_x is the radial component of the solar wind velocity at the negative IMF B_z component) for the instant when *Dst* was minimal.

All moderate and strong magnetic storms with $Dst \le -50$ nT registered in 1976–2000 were divided into eight groups depending on the stream type that caused these storms. As a result, it was found that 43 magnetic storms were related to MCs, 86 storms were related to CIR, 95 storms were related to Ejecta, 56 storms were related to the Sheath before Ejecta (Sh_E), 8 storms were related to the Sheath before MC (Sh_{MC}), 64 storms were related to all Sheath events before ICME (Sh_{MC} + Sh_E), 138 storms were related to all ICMEs (MC + Ejecta), and 75 magnetic storms were related to an indeterminate type of the solar wind stream (IND). The indeterminate type included the events for which it was impossible to reliably identify the stream type, or some parameters were absent, or the phenomenon type was complex.

Note that we did not perform a linear approximation when the number of events was smaller than 10 because reliability for a small number of events (e.g., for Sh_{MC} when we analyzed the dependence of *AE* and *Dst* on E_y, *Pd*, and IMF σB). When the number of

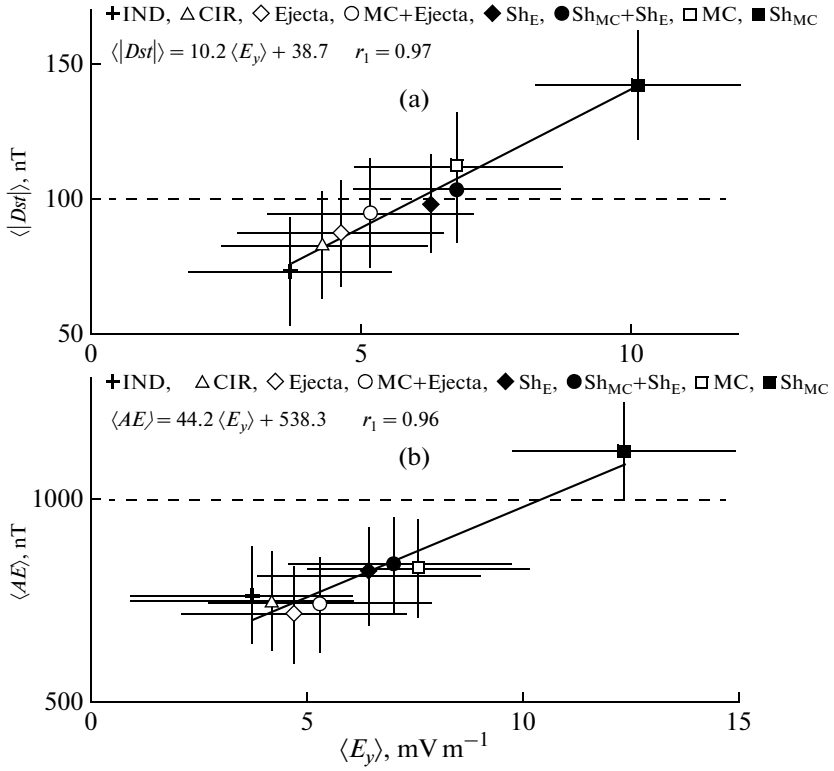

Fig. 1. The dependence of the (a) $\langle|Dst|\rangle$, and (b) $\langle AE\rangle$ indices on the $\langle E_y\rangle$ field averaged for the solar wind types marked by different symbols: IND, CIR, Ejecta, MC + Ejecta, Sh_E, Sh_{MC} + Sh_E, MC, and Sh_{MC}. Vertical and horizontal bars crossing each point show the rms deviation. Solid lines show the regression lines. The regression equations and the linear correlation coefficients (r_1) are presented at the top of each panel.

events was smaller than 30, we did not perform a quadratic approximation (e.g., for MC events when we analyzed the dependence of AE on E_y). For a quadratic empirical dependence, when the deviation from the linear dependence is characterized by a small number of points (e.g., one point locating far from the area of points), we performed an approximation by a broken line from two linear segments: segment 1 included many points, and segment 2 included the last two points from segment 1 plus these isolated points.

3. ANALYSIS RESULTS

Figure 1 presents the dependence of the geomagnetic indices averaged for each solar wind type on the average electric field $\langle E_y\rangle$: (a) $\langle|Dst|\rangle$ and (b) $\langle AE\rangle$. Different types of the solar wind stream are shown by different symbols (the corresponding denotations are presented above each plot). Vertical and horizontal bars crossing points show the rms deviation. The linear correlation coefficient (r_1) and regression equation (shown by a solid line) are presented at the top of each panel.

Figure 1 indicates the average intensity of magnetic storms and substorms during storms caused by different solar wind streams and the relationship of this intensity to the average electric field value $\langle E_y\rangle$. We can assume that Sh_{MC} are the most geoeffective streams according to the average electric field value $\langle E_y\rangle$ since these streams mainly result in intense magnetic storms ($|Dst| > 100$ nT) and strong auroral currents ($AE >$ 1000 nT) [Echer et al., 2006]. The same events (Sh_{MC}) have the largest electric field values ($\langle E_y\rangle > 10$ mV m^{-1}). Also strong magnetic storms with $Dst < -100$ nT but with moderate auroral currents ($500 < AE < 1000$ nT) are caused by Sheath before Ejecta (Sh_E) and ICME (Sh_{MC} + Sh_E) and by MCs themselves. These three types of events have the smaller (by a factor of 1.5–2) average values of the electric field ($\langle E_y\rangle = 6$–8 mV m^{-1}). Events (MC + Ejecta) are at the geoeffectiveness boundary between strong and moderate magnetic storms with moderate auroral currents ($500 < AE <$ 1000 nT). Ejecta and especially CIR events are mostly related to moderate magnetic storms and moderate auroral currents. Both types of events have even smaller $\langle E_y\rangle$ values: > 4 and < 5 mV m^{-1}, respectively. According to the values of the indices, IND events are less geoeffective and are mostly related to moderate storms and moderate auroral electrojet currents. The smallest average value of the electric field ($\langle E_y\rangle \sim$ 4 mV m^{-1}) corresponds to this type of events. Thus,

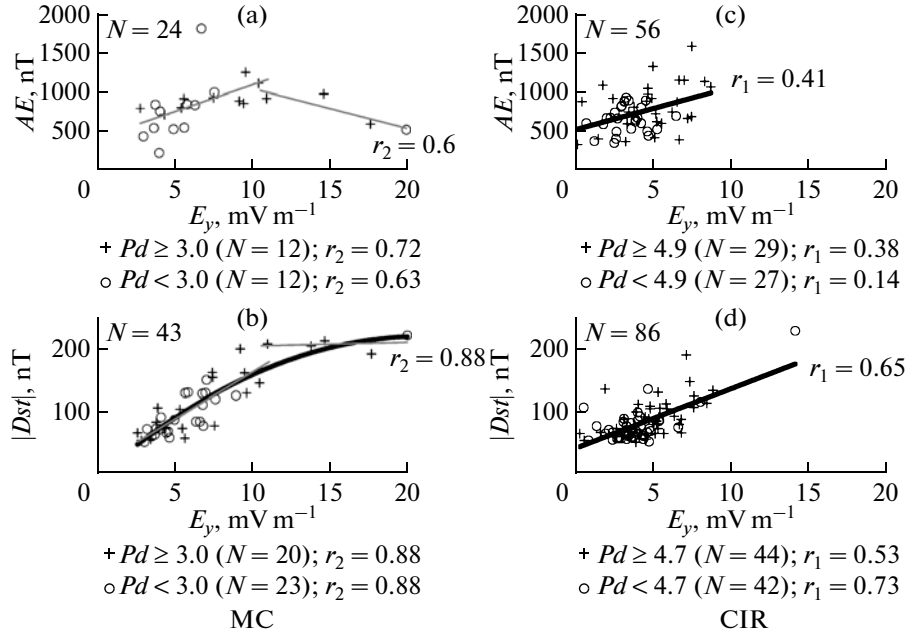

Fig. 2. The dependence of the (b), (d) $|Dst|$ and (a), (c) AE geomagnetic indices on the electric field value E_y for (a), (b) MC and (c), (d) CIR events.

each solar wind type is possibly characterized by its own average value of the electric field E_y and $|Dst|$ and AE indices.

The dependence of the AE and $|Dst|$ geomagnetic indices on the electric field value E_y is shown in Figs. 2–5 separately for each group of magnetic storms related to the specific type of the solar wind stream. Solid lines show an approximation of the dependence or regression lines with the correlation coefficient values (r_1 and r_2 are the linear and quadratic correlation coefficients, respectively).

Figure 2 shows the dependence of the (a), (c) AE and (b), (d) $|Dst|$ indices on E_y for (a), (b) MCs and (c), (d) CIR events. Figures 2a and 2b indicate that the AE and Dst indices nonlinearly depend on the electric field E_y for MCs (the quadratic correlation coefficients are high: $r_2 = 0.6$ and 0.88, respectively). We can assume that the values of the AE and $|Dst|$ indices linearly increase at small field values ($E_y < 11$ mV m^{-1}). However, at large E_y values (>11 mV m^{-1}), the AE index decreases and the $|Dst|$ index remains unchanged, i.e., indices are saturated. For clearness, we present in Fig. 2a an approximation of the AE dependence on E_y by a broken line including two linear segments (thin lines): segment 1 corresponds to $E_y < 11$ mV m^{-1} (the regression line constructed based on 21 points $AE = 67.8E_y + 429.3$); segment 2, to $E_y >$ 10.5 mV m^{-1} (the regression line for four points $AE = -50.9E_y + 1568.4$). Figure 2b similarly shows an approximation of the $|Dst|$ dependence by a broken line composed of two linear segments (thin lines): segment 1 with $E_y < 11$ mV m^{-1} (the regression line constructed using 39 points $|Dst| = 15.1E_y + 14.7$); segment 2 with $E_y > 10.5$ mV m^{-1} (the regression line for five points $|Dst| = 0.59E_y + 200.9$). For CIR events, the AE index is almost independent of the electric field value (the linear correlation coefficient is low $r_1 =$ 0.41), whereas the $|Dst|$ index linearly increases with increasing electric field E_y with a correlation coefficient of $r_1 = 0.65$, which indicates that these parameters are closely related to each other (Figs. 2c, 2d).

Figure 3 shows the dependence of the AE (Figs. 3a, 3c) and $|Dst|$ (Figs. 3b, 3d) indices on the E_y field values observed in Ejecta events (Figs. 3a, 3b) and in the Sheath before these events (Sh_E; Figs. 3c, 3d). Figure 3a indicates that the AE index is independent of the electric field value for Ejecta events (the correlation coefficient is low $r_2 = 0.45$). At the same time, the $|Dst|$ index linearly increases with increasing E_y, and the linear correlation coefficient is high $r_1 = 0.82$ (see Fig. 3b). For clearness, in Fig. 3a we show the linear approximation in two electric field intervals by thin straight lines: interval 1 for $E_y < 11$ mV m^{-1} with the regression line constructed based on 68 points $AE = 50.6E_y + 493.56$; interval 2 corresponds to $E_y >$ 9 mV m^{-1} with the regression line constructed based on three points $AE = -130.1E_y + 2255.4$. It is clear that the AE index tends to decrease with increasing $E_y > 11$ mV m^{-1} as for MC events; however, the statistics of Ejecta events is too insufficient and the correlation coefficient is low ($r_2 < 0.5$). Figures 3c and 3d

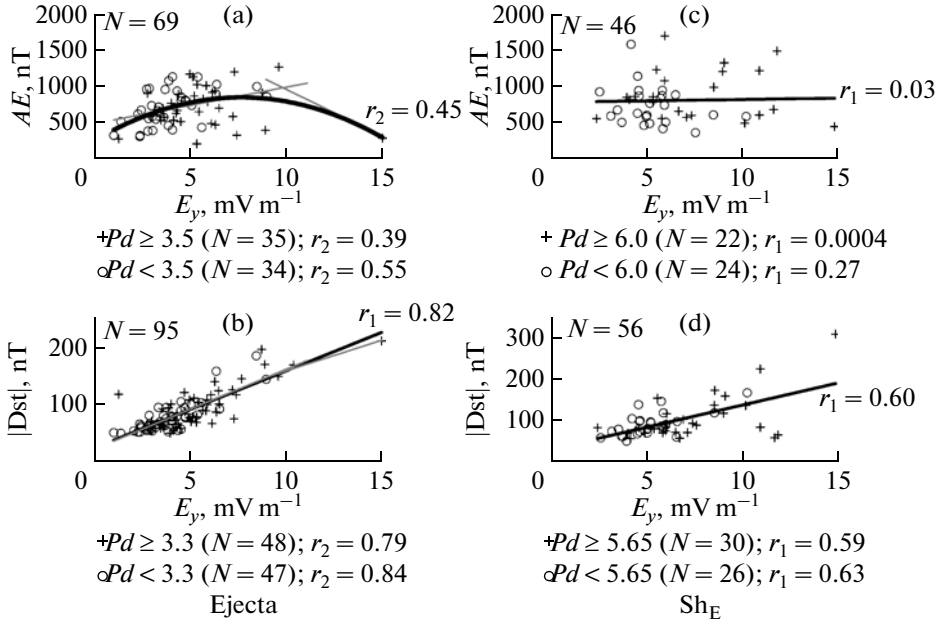

Fig. 3. The dependence of the (b), (d) $|Dst|$ and (a), (c) AE indices on the electric field value (E_y) for (a), (b) Ejecta and (c), (d) Sheath before Ejecta (Sh_E).

indicate that strong electric fields with $E_y > 11$ mV m^{-1} are more frequently registered in the Sheath before Ejecta (Sh_E) than in the Ejecta region (seven and one events, respectively). For Sh_E events, the AE index is independent of the E_y field value (the correlation coefficient is low $r_1 = 0.03$); at the same time, the $|Dst|$ index linearly increases with increasing E_y field and the correlation coefficient is high $r_1 = 0.6$ (see Figs. 3c, 3d).

Figures 4a and 4b show the dependence of the AE and $|Dst|$ indices on the electric field E_y for Sheath before MC (Sh_{MC}). Although the linear correlation coefficients are high ($r_1 = 0.76$ and 0.86, respectively), the statistical significance of the result is low, since such events are rare. Figures 4c and 4d show the same for Sheath before all ICMEs ($Sh_{MC} + Sh_E$). It is evident that the AE index is independent on the E_y field for the ($Sh_{MC} + Sh_E$) sum of events and Sh_E events (the correlation coefficient is low $r_1 = 0.33$). At the same time, the $|Dst|$ index linearly increases with increasing electric field for these events (the correlation coefficient is high $r_1 = 0.7$).

Figures 5a and 5b show the same for all ICME events, i.e., for MC + Ejecta. It is clear that the AE index is independent of the electric field (the quadratic correlation coefficient is $r_2 = 0.47$). The AE index dependence is approximated by a broken line composed of two linear segments: segment 1 corresponds to $E_y < 11$ mV m^{-1} with the regression line constructed for 89 points $AE = 60.9E_y + 455.0$; segment 2 corresponds to $E_y > 10$ mV m^{-1} with the regression line constructed for five points $AE = -57.5E_y + 1545.6$ and indicates that the AE index tends to increase at $E_y <$ 10–11 mV m^{-1} and subsequently decreases when $E_y >$ 11 mV m^{-1} as in MC events. At the same time, the $|Dst|$ index linearly increases with increasing E_y for the same MC + Ejecta events (the linear correlation coefficient is $r_1 = 0.78$). For illustration, Fig. 5b also shows an approximation by a broken line composed of two linear segments (gray lines): segment 1 with $E_y < 11$ mV m^{-1} (the regression line constructed for 134 points $|Dst| = 12.9E_y + 29.1$); segment 2 with $E_y > 10.5$ mV m^{-1} (the regression line constructed based on five points $|Dst| = 0.67E_y + 198.8$). The statistics of the events with $E_y >$ 11 mV m^{-1} are insignificant (eight MC + Ejecta events have the E_y field larger than 10 mV m^{-1}); therefore, we can only state that the ring current intensity tends to saturate when the E_y electric fields are large. Figures 5c and 5d show the same for IND events. For these events, the AE index value is independent of the E_y field; at the same time, the $|Dst|$ index linearly depends on the electric field with a high correlation coefficient ($r_1 = 0.70$).

To verify the possible effect of the variations in the solar wind dynamic pressure Pd and in the level of IMF σB fluctuations on the dependence of the indices on the E_y field, we divided each type of event into two subgroups depending on the Pd value (circles for a low dynamic pressure $Pd < P_0$ and crosses for a high pressure $Pd \geq P_0$, where P_0 is the dynamic pressure threshold value shown in the captions below Figs. 2–5) and on the IMF σB value (circles for a low fluctuation level

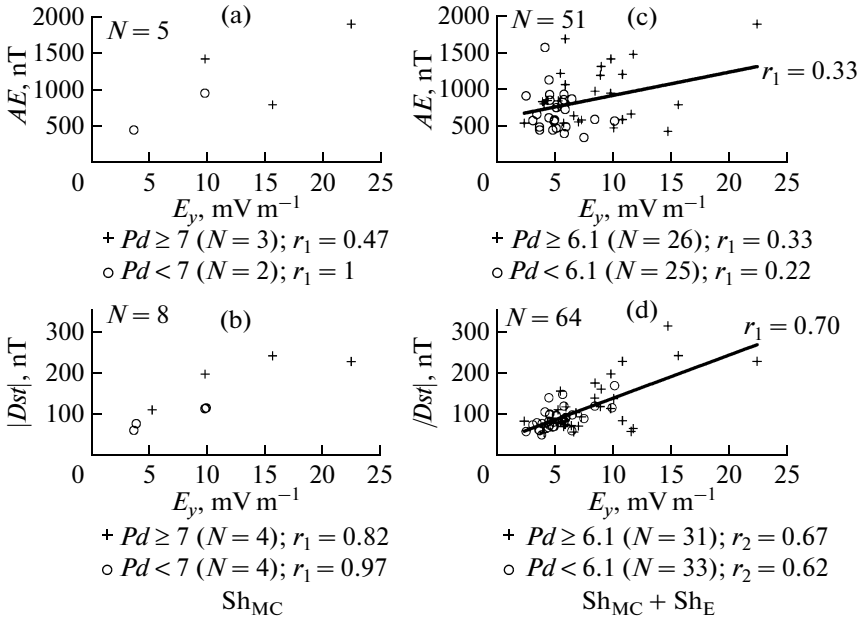

Fig. 4. The dependence of the (b), (d) $|Dst|$ and (a), (c) AE indices on the electric field value E_y for the following events: (a), (b) Sheath before MC (Sh_{MC}) and (c), (d) all Sheaths ($Sh_E + Sh_{MC}$).

$\sigma B < \sigma B_0$ and crosses for considerable fluctuations $\sigma B \geq \sigma B_0$, where σB_0 is the threshold value of the IMF fluctuation level shown below Figs. 6–9). The P_0 and σB_0 threshold values used to divide the interval were determined approximately so that the number of points in each subgroup would be identical or change insignificantly.

For either subgroup with a high (crosses) and low (circles) pressure Pd, we determined the regression lines (not shown for shortness) and estimated the correlation coefficients, the values of which are presented at the bottom of Figs. 2–5. An analysis of the subgroups with different dynamic pressure values gave the following results. First, a higher dynamic pressure $Pd > P_0$ (compare circles and crosses in Figs. 2–5) is mostly observed at strong electric fields ($E_y > 10$ mV m^{-1}) for all stream types (e.g., MC, Sh_{MC}, Ejecta, Sh_E, MC + Ejecta, $Sh_{MC} + Sh_E$, and IND) except CIR. At the same time, both low and high Pd values are observed at weaker fields ($E_y < 10$ mV m^{-1}). Second, the correlation coefficient between the $|Dst|$ index and field E_y is higher in the subgroup with low pressure ($Pd < P_0$) than in the subgroup with high pressure ($Pd > P_0$) or in the entire sample for some types of events (CIR, Ejecta, Sh_E, and Sh_{MC}). In contrast, the correlation is higher in the subgroup with high pressure ($Pd > P_0$) for other types of events ($Sh_{MC} + Sh_E$, MC + Ejecta, and IND).

A similar analysis for each type of events was performed for the subgroups with high ($\sigma B \geq \sigma B_0$) and low ($\sigma B < \sigma B_0$) levels of IMF σB fluctuations. The solid lines in Figs. 6–9 show the regression lines for all events (i.e., repeating Figs. 2–5), and the dotted lines show the regression lines for the subgroup with high ($\sigma B \geq \sigma B_0$, crosses) and low ($\sigma B < \sigma B_0$, circles) levels of IMF σB fluctuations. It is clear that strong electric fields ($E_y > 10$ mV m^{-1}) are accompanied by a higher level of fluctuations for the MC, Sh_{MC}, MC + Ejecta, and $Sh_{MC} + Sh_E$ events. A comparison of the correlation coefficients for the subgroups with different levels of IMF σB fluctuations indicates that considerable IMF σB fluctuations make the relationship between the AE index and field E_y slightly closer for some types of events (e.g., MC, Sh_E, $Sh_{MC} + Sh_E$, MC + Ejecta, and IND) and between the $|Dst|$ index and E_y (for Sh_E, $Sh_{MC} + Sh_E$, and IND events).

To quantitatively verify the assumptions that high pressure ($Pd \geq P_0$) and considerable IMF fluctuations ($\sigma B \geq \sigma B_0$) can affect the dependence of the geomagnetic indices on the E_y field during magnetic storms, we estimated the deviations of the AE and Dst indices from the regression lines for the groups with high and low Pd and with high and low levels of IMF σB fluctuations. The results of these calculations and the number of events in either subgroup are presented in Figs. 10a–10c and Figs. 10d–10f for the $|Dst|$ and AE indices, respectively.

Figures 10b and 10e indicate that the $|Dst|$ and AE indices deviate from the regression line for the subgroups with considerable ($\sigma B \geq \sigma B_0$) and insignificant ($\sigma B < \sigma B_0$) IMF fluctuations, respectively. Figures 10c and 10f show the same for the subgroups with high

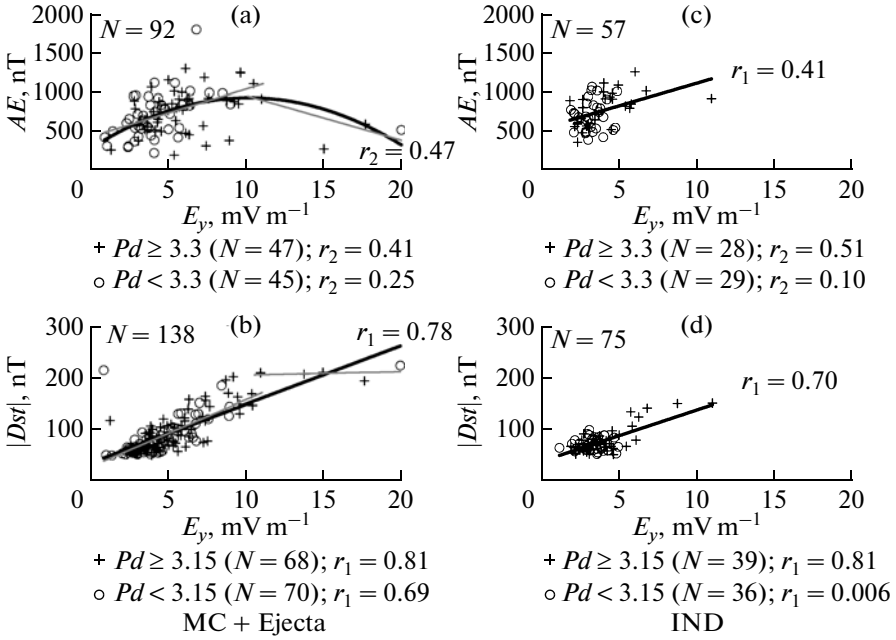

Fig. 5. The dependence of the (b), (d) $|Dst|$ and (a), (c) AE indices on the electric field value E_y for the following events: (a), (b) all ICMEs (MC + Ejecta) and (c), (d) solar wind of an indeterminate type (IND).

($Pd > P_0$) and low ($Pd < P_0$) dynamic pressures, respectively. An analysis of Fig. 10 indicates that the average deviations of both indices from the main dependence in either subgroup are substantially smaller than the rms deviations for all types of streams except Sh_{MC}, the number of which is too small.

4. DISCUSSION OF RESULTS

The correlation between the solar wind parameters and geomagnetic indices has been analyzed in many works [Snyder et al., 1963; Gonzalez et al., 1998; Badruddin, 1998; Wang et al., 2003; Kane, 2005] (see also [Yermolaev et al., 2007b] and references therein). However, only some works took account of the solar wind stream type that caused a storm.

Our results confirm that the dusk-dawn electric field E_y component is mainly responsible for the values of the $|Dst|$ and AE indices during moderate and strong magnetic storms, i.e., being the main geoeffective factor. On average, the E_y field can differ for different solar wind stream types, which depends on the stream formation physics and criteria of selection of different stream types. The dependence of the $|Dst|$ index on pressure in some solar wind types is related to the fact that pressure directly correlates with field E_y in these solar wind types. That is, the index may actually depend only on one independent parameter E_y and indirectly depends on pressure.

All information on the dependences of the AE and $|Dst|$ indices on the electric field E_y we obtained, including the regression equations and linear (r_1) and quadratic (r_2) correlation coefficients, for eight types of geoeffective solar wind events is presented in Tables 1 and 2, respectively. The results (linear and quadratic approximations with correlation coefficients) obtained in [Kershendolts et al., 2007] are given in an individual raw (marked by *). Note that the authors of this work included all ICMEs and Sheath before them in the MC events. Nevertheless, it is clear that their approximations are similar to our dependences of $|Dst|$ on E_y for the CIR and MC types of streams.

An analysis of the correlation confirms that the value of the $|Dst|$ index depends on the electric field value E_y during a magnetic storm for all eight types of solar wind streams: the correlation coefficient is significant (>0.5) and varies from 0.6 for Sh_E events to 0.86 for MC and Sh_{MC} events. Since the number of Sh_{MC} events we analyzed is too small (five events, see Table 2), the reliability of the correlation coefficient between the storm intensity $|Dst|$ and electric field E_y obtained for these events is low in spite of the fact that the correlation coefficient value is large ($r_1 = 0.86$). For the remaining stream types, we can assume that the closest relationship between the $|Dst|$ index and electric field E_y is observed for the ICME events: $r_1 =$ 0.86, 0.82, and 0.78 for MCs, Ejecta, and their sum (MC + Ejecta), respectively. The relationship between E_y and $|Dst|$ is less close for all compressed regions, including the Sheath and CIR, and for IND events: $r_1 = 0.7$ for all Sheaths and $Sh_E + Sh_{MC}$, $r_1 = 0.7$ for IND events, $r_1 = 0.65$ for CIRs, and $r_1 = 0.6$ for Sh_E.

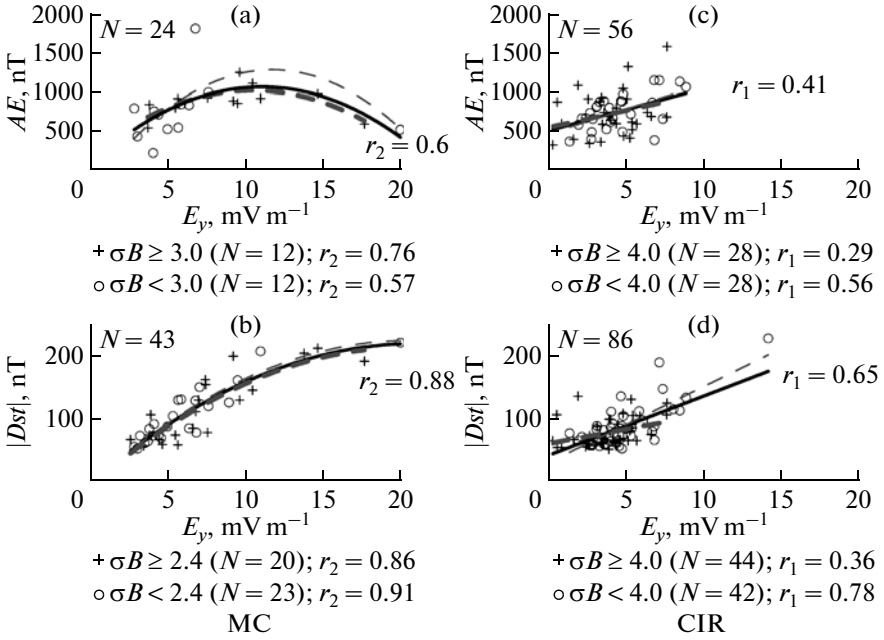

Fig. 6. The same as in Fig. 2 but points are divided according to the IMF σB fluctuation.

Although the differences between the correlation coefficient values are insignificant, we can assume that the observed effect is related to a more regular behavior of B_z (and E_y) in ICMEs since a magnetic storm "remembers" previous B_z (and E_y) values [Yermolaev et al., 2010b].

The values of the correlation coefficients we obtained agree with the published data for individual types of events. For example, Kane [2005] considered the relationship between the *Dst* index minimum and the electric field (*VBs*) for moderate and strong magnetic storms (59 magnetic storms for 1973–2003, the *Dst* scale from −50 to −500 nT). A correlation coefficient of 0.67 was obtained as a result of an analysis performed independently on the solar wind stream type [Kane, 2005], which is close to the values we obtained for the Sheath and CIR compressed regions and indeterminate events.

An analysis of 64 intense magnetic storms ($Dst \le -85$ nT) registered by the ACE satellite in 1997–2002, performed independently on the source type in the solar wind, indicated that the peaks of the electric field E_y correlate with the *Dst* index minimum (the correlation coefficient is $r = 0.87$) [Gonzalez and Echer, 2005], which is close to our data obtained for MCs. Vivek, Gupta and Badruddin [2009] analyzed 88 intense magnetic storms with $Dst < -100$ nT (to −370 nT) during cycle 23, caused by five different types of the solar wind streams. However, the dependence of the *Dst* index on E_y is presented for all powerful storms independently on the stream type that caused this storm. The relationship between *Dst* peaks and E_y is linear ($Dst = -77.40E_y - 7.85$) and is characterized by a high correlation coefficient, which also almost coincides with the values we obtained for MCs. We should note that about 18 of 88 events had large electric field values ($E_y > 10$ mV m^{-1}). However, Vivek Gupta and Badruddin [2009] considered only the linear relationship between E_y and the *Dst* index (rather than the quadratic or piecewise linear dependence for MCs in our work and in [Kershendolts et al., 2007]). This is possibly related to the fact that strong magnetic storms were caused by the "mixture" of streams (i.e., ICMEs interacting with one another [Yermolaev and Yermolaev, 2008]) rather than by their individual types.

The relationship between the *Dst* index and E_y for CIR was studied in [Alves et al., 2006; Zhang et al., 2008]. It was indicated that the *Dst* index linearly depends on E_y ($Dst = -11.1E_y - 11.3$ [Zhang et al., 2008]; i.e., the regression line is close to our line for CIR (see Table 2). The correlation coefficient obtained in [Alves et al., 2006] for CIR ($r_1 = 0.66$) almost coincides with the value ($r_1 = 0.65$) that we obtained for these events. Cane et al. [2000] also obtained a linear relationship between the maximal southward IMF and the *Dst* index with a correlation coefficient of $r = 0.74$ for the Ejecta events with the Sheath before them (Ejecta + Sheath), which is close to the correlation coefficient (0.78) that we obtained for all ICMEs (MC + Ejecta). Wu and Lepping [2002] studied the relationship between the magnetic storm intensity (the *Dst* minimum) and the electric field E_y component for 34 MCs during 1995–1998. The

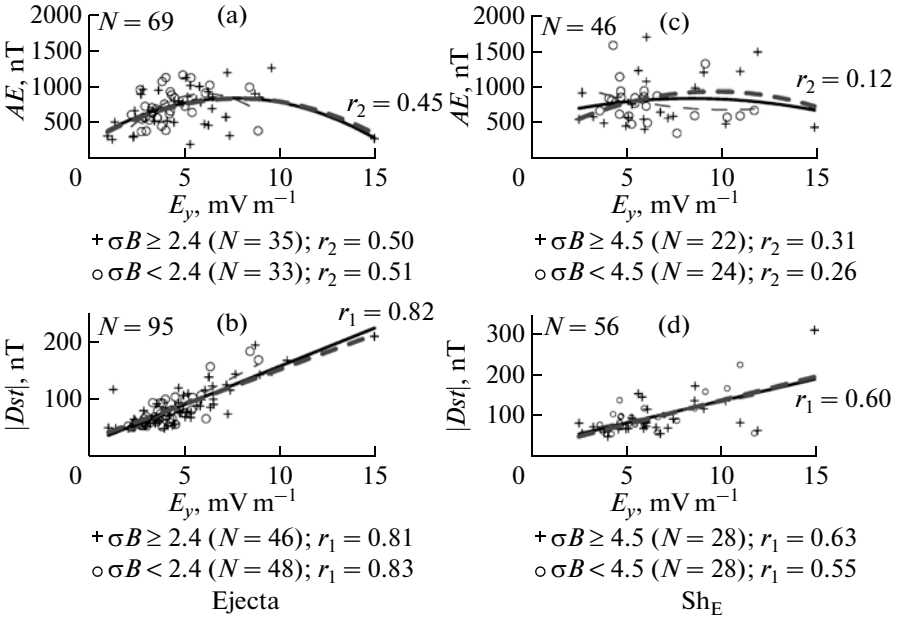

Fig. 7. The same as in Fig. 3 but points are divided according to the IMF σB fluctuation.

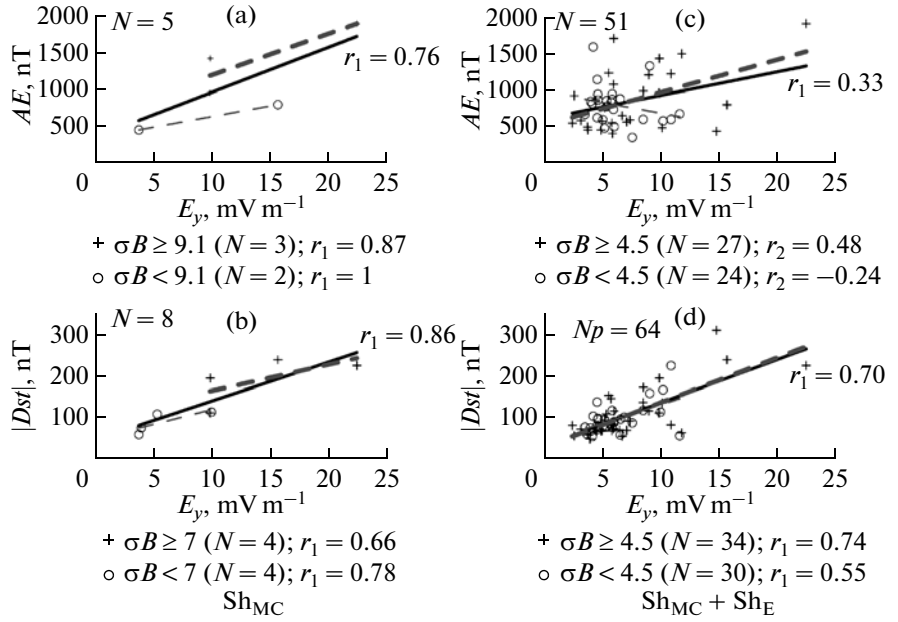

Fig. 8. The same as in Fig. 4 but points are divided according to the IMF σB fluctuation.

authors used only the linear relationship between the storm intensity and the electric field within MCs and obtained a correlation coefficient of $r_1 = 0.79$, which is slightly smaller than the value that we obtained for MCs ($r_1 = 0.86$) but almost coincides with the correlation coefficient ($r = 0.78$) that we obtained for all ICMEs (Ejecta + MC). Note that about five MCs had strong fields ($E_y > 10$ mV m^{-1}); however, the relationship between the parameters was described only by a linear dependence [Wu and Lepping, 2002]. A smaller value of the correlation coefficient for MCs than such a value that we obtained is possibly explained by this fact.

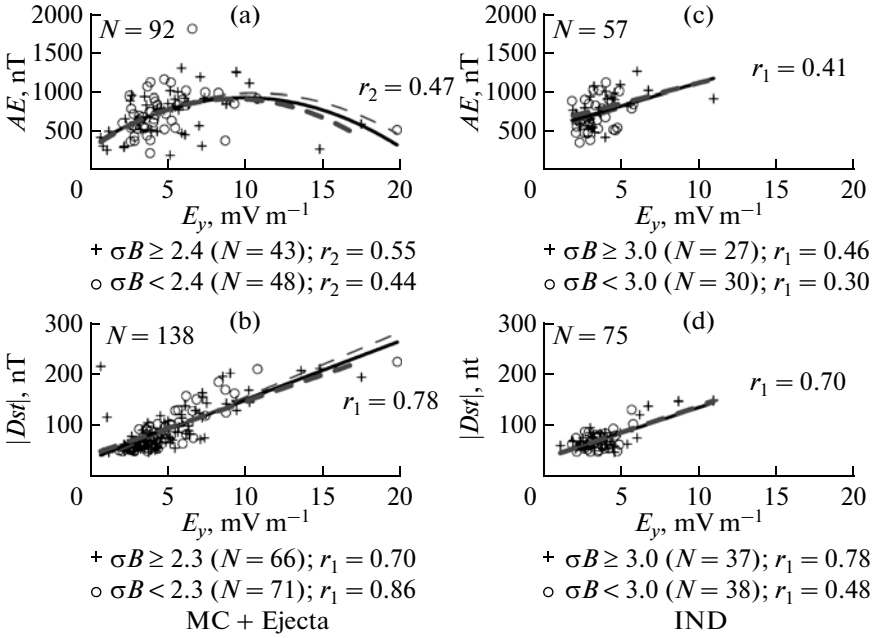

Fig. 9. The same as in Fig. 5 but points are divided according to the IMF σB fluctuation.

The results of our analysis indicate that the ring current intensity $|Dst|$ possibly nonlinearly depends on the electric field E_y component for MCs and maybe all ICMEs (MC + Ejecta): the quadratic correlation coefficients are high for these events. Specifically, the ring current linearly increases with increasing electric field when its values are small ($E_y < 11$ mV m^{-1}); however, at large field values ($E_y > 11$ mV m^{-1}), the saturation of the $|Dst|$ index is observed when the ring current intensity remains unchanged. A similar character of the relationship between the $|Dst|$ index and E_y was obtained in [Kershendolts et al., 2007; Plotnikov and Barkova, 2007] for MCs with the Sheath before them (Sh_{MC}). Our results for MCs and possibly all ICMEs confirm the conclusion on the behavior of the indices for large electric fields ($E_y > 12$ mV m^{-1}) drawn by these researchers. Tables 1 and 2 indicate that the *AE* and $|Dst|$ indices are related to E_y by the quadratic dependence for MCs, which is close to the regression lines in [Kershendolts et al., 2007; Plotnikov and Barkova, 2007] and has close correlation coefficients for the *AE* $r_2 = 0.7$ (0.6 in our work) and $|Dst|$ $r_2 = 0.9$ (0.88 in our work) indices. The CIR events are also characterized by a similar linear dependence of the *Dst* index on E_y with similar correlation coefficients $r_1 = 0.65$ (0.7 in our work). Our results achieved for CIR events substantially differ from the data obtained in [Kershendolts et al., 2007; Plotnikov and Barkova, 2007]: $r_1 = 0.41$ and 0.6, respectively; and the relationship between the *AE* index and the E_y field is absent. Moreover, according to our data, the *AE* index is independent of (or weakly depends on) the electric field E_y component for almost all event types except rare Sh_{MC} events (i.e., including CIRs). The differences can be explained by different CIR selection criteria.

An important result of our work consists determining that the dynamic pressure *Pd* and the level of IMF σB fluctuations do not affect the dependence of the $|Dst|$ index during magnetic storms (the *Dst* minimum during the storm main phase) on the electric field E_y. We can assume that both geomagnetic indices do not depend on the dynamic pressure and IMF fluctuation level but possibly affect the scatter of points (the value of uncertainty). Additional studies should be performed in order to make a final conclusion.

This conclusion partially agrees with other works, which indicated that the contribution of *Pd* to the *Dst* index decreases with increasing geoeffective component of the electric field (E_y) [O'Brien and McPherron, 2000, 2002; McPherron and O'Brien, 2001]. Specifically, the coefficient before the dynamic pressure $b(E)$, which was used to calculate the corrected *Dst** index in the formula presented in [Burton et al., 1975], is not constant. This coefficient decreases by a factor of five when the electric field E_y increases from 0 to 18 mV m^{-1} [O'Brien and McPherron, 2000, 2002; McPherron and O'Brien, 2001; Siscoe et al., 2005]. Consequently, the correction for *Dst*, related to an increase in the dynamic pressure during the magnetic storm main phases, is possibly smaller than is usually assumed in the formula [Burton et al., 1975; Siscoe et al., 2005], which indirectly agrees with the data we obtained. This is caused by a change in the current structure within the magnetosphere–ionosphere system. MHD modeling indicates [Siscoe et al., 2002a;

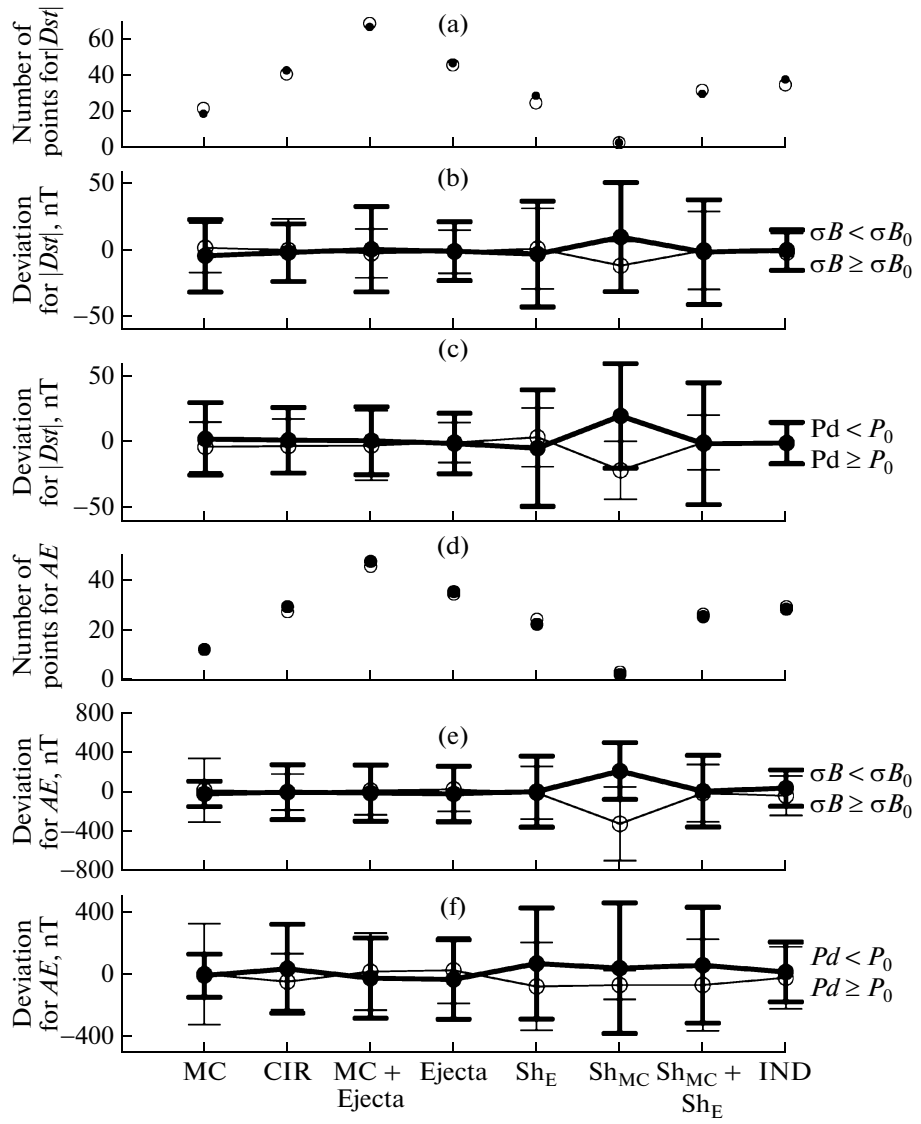

Fig. 10. The number of points and the deviation of the (a)–(c) $|Dst|$ and (d)–(f) AE indices from the regression lines for different subgroups of events with $Pd < P_0$ (thin line) and $Pd \geq P_0$ (thick line) (c), (f) and for the subgroups of events with $\sigma B < \sigma B_0$ (thin line) and $\sigma B \geq \sigma B_0$ (thick line) (b), (e). Vertical bars show rms deviations. Panels (a) and (d) show the number of points in either subgroup for the $|Dst|$ and AE indices, respectively.

White et al., 2001] that the Chapman–Ferraro (C–F) current system is replaced by the region 1 current system when IMF has a strong southward component and a large electric field (B_z ~20 nT, $E_y > 10$ mV m^{-1}). When the E_y electric fields are large, the region 1 current increases with increasing solar wind pressure Pd [Siscoe et al., 2002b]. We factually have two modes of interaction between the solar wind and the magnetosphere: mode 1 (when the solar wind and C–F currents predominate) and mode 2 (when the ionosphere and region 1 currents predominate [Vasyliunas, 2004]). The dimensionless quantity ($\mu_0 \Sigma_p V_A \varepsilon$), which can be larger and smaller than unity, is responsible for this division. Here Σ_p is the ionospheric Pedersen conductance, V_A is the Alfvén velocity, and ε is the effectiveness of reconnection at the magnetopause, determined as a ratio of the reconnection potential to the maximum possible potential drop that can be imposed by the solar wind on the magnetosphere [Siscoe et al., 2005]. The magnetosphere demonstrates both interaction types. Most of the time the interaction with the magnetosphere determined by the solar wind (i.e., dynamic pressure). However, the ionospheric mode predominates during the interaction with the magnetosphere (i.e., zone 1 currents predominate) during magnetic storms, when the Alfvén velocity (V_A) is high and the effectiveness of reconnection at the magnetopause (ε) is maximal. That is, when IMF has a strong southward component ($E_y > 10$ mV m^{-1}), which takes

Table 1. Equations of regression between AE and E_y and the linear (r_1) and quadratic (r_2) correlation coefficients for different types of solar wind

SW type	Number of points	Regression equations	Correlation coefficient r_1	Correlation coefficient r_2
MC	24	$AE = 110.5 + 176.8E_y - 8.04E_y^2$ $AE = 780.0 + 6.8E_y$	0.1	0.6
MC*	35	$AE = 137.7 + 186.9\ E_y - 7.4E_y^2$	0.4	0.7
CIR	56	$AE = 526.5 + 53.7E_y$ $AE = 610.2 + 6.56E_y + 5.3E_y^2$	0.41	0.42
CIR*	38	$AE = 819.5 + 34.3E_y$	0.6	0.4
MC + Ejecta	92	$AE = 309.9 + 126.8E_y - 6.3E_y^2$ $AE = 646.3 + 18.3E_y$	0.20	0.47
Ejecta	69	$AE = 266.3 + 155.4E_y - 10.28E_y^2$ $AE = 612.5 + 22.3E_y$	0.19	0.45
Sh_E	46	$AE = 576.4 + 66.2E_y - 3.96E_y^2$ $AE = 785.5 + 3.87E_y$	0.03	0.12
Sh_{MC}	5	$AE = 364.8 + 60.99E_y$	0.76	
$Sh_{MC} + Sh_E$	51	$AE = 618.1 + 31.7E_y$ $AE = 803.4 - 13.87E_y + 2.39E_y^2$	0.33	0.38
IND	57	$AE = 545.4 + 58.4E_y$ $AE = 353.3 + 143.9E_y - 7.87E_y^2$	0.41	0.45

Note: Symbol * means that the data on this raw were taken from [Kershendolts et al., 2007].

Table 2. Equations of regression between $|Dst|$ and E_y and correlation coefficients r_1 and r_2 for different types of solar wind

SW type	Number of points	Regression equations	Correlation coefficient r_1	Correlation coefficient r_2
MC	43	$\|Dst\| = -2.19 + 21.45E_y - 0.51E_y^2$ $\|Dst\| = 35.78 + 11.27E_y$	0.86	0.88
MC*	35	$\|Dst\| = -83.1 + 31.9E_y - 0.8E_y^2$	0.8	0.9
CIR	86	$\|Dst\| = 66.81 - 1.29E_y + 0.96E_y^2$ $\|Dst\| = 42.11 + 9.57E_y$	0.65	0.72
CIR*	38	$\|Dst\| = 31.8 + 9.8E_y$	0.7	0.5
MC + Ejecta	138	$\|Dst\| = 30.1 + 13.4E_y - 0.12E_y^2$ $\|Dst\| = 36.39 + 11.32E_y$	0.78	0.78
Ejecta	95	$\|Dst\| = 25.63 + 13.39E_y$ $\|Dst\| = 32.01 + 10.92E_y + 0.19E_y^2$	0.82	0.83
Sh_E	56	$\|Dst\| = 30.1 + 10.8\ E_y$ $\|Dst\| = 13.44 + 19.04 - 0.84E_y^2$	0.60	0.64
Sh_{MC}	8	$\|Dst\| = 48.21 + 9.28E_y$	0.86	
$Sh_{MC} + Sh_E$	64	$\|Dst\| = 33.85 + 10.32E_y$ $\|Dst\| = 36.96 + 9.51E_y - 0.03E_y^2$	0.70	0.70
IND	75	$\|Dst\| = 37.0 + 9.92E_y$ $\|Dst\| = 57.19 + 0.71E_y + 0.86E_y^2$	0.70	0.73

Note: Symbol * means that the data on this raw were taken from [Kershendolts et al., 2007].

place at the peak of the magnetic storm main phase (at the *Dst* index minimum), the C–F current system, which increases the *Dst* value (makes it less negative), is replaced by the region 1 current system, which is neutral with respect to the *Dst* index value [White et al., 2001; Siscoe et al., 2002a, 2005; Vasyliunas, 2004].

We emphasize that substorm activity *AE* during magnetic storms depending on the value of the solar wind electric field E_y was not studied previously for many different types of solar wind streams. The studies of eight different types of solar wind streams indicate that the auroral current intensity (the *AE* index)

depends on the E_y electric field value (the correlation coefficient is > 0.5) only for MCs and the Sheath before them (Sh_{MC}). For the remaining types of solar wind streams, the auroral current (the *AE* index) is independent on the E_y electric field value or this dependence is weak (the correlation coefficient is <0.5).

The relationship between the *AE* index (auroral activity) and the IMF B_z component has long been known [Arnoldy, 1971; Meng et al., 1973; Baker et al., 1983; Weimer et al., 1990]. A statistical comparison of the *AE* index values with the IMF B_z component during powerful geomagnetic storms (independently of the storm source type) indicated that the *AE* index tends to saturate (to a fixed *AE* value of ~1100 nT) when the electric fields are strong ($E_y > 10$ mV m^{-1}) [Weimer et al., 1990]. According to our data for MC events, during magnetic storms the *AE* index first monotonously increases to a certain maximal value of 1000–1100 nT when the electric field is $E_y < 11$ mV m^{-1}, which coincides with the data obtained in [Weimer et al., 1990]. However, when this index becomes saturated, its value decreases at a subsequent increase in the field ($E_y > 11$ mV m^{-1}), which differs from the result achieved in [Weimer et al., 1990]. This decrease is possibly related to the fact that the auroral electrojet moves equatorward during magnetic storms, and polar stations that are used to determine the *AE* index do not register it.

The saturation of the *AE* index is caused by the fact that the polar cap potential becomes saturated because the magnetosphere–ionosphere coupling is the nonlinear process [Weimer et al., 1990]. The modeling of the magnetosphere–ionosphere coupling indicates that the level of the polar cap potential saturation decreases with increasing conductivity of the auroral ionosphere caused by diffuse precipitation [Weimer et al., 1990].

5. CONCLUSIONS

Using our Solar Wind Catalog created based on the OMNI database for 1976–2000, we analyzed the dependence of the *Dst* and *AE* geomagnetic indices (the intensities of the ring and auroral currents) on the value of the solar wind electric field E_y and dynamic pressure *Pd* and the level of IMF σB magnetic fluctuations during the main phase of moderate and strong magnetic storms caused by different types of solar wind streams: CIR, MC, Sh_{MC}, Ejecta, Sh_E, MC + Ejecta, $Sh_{MC} + Sh_E$, and IND.

We distinguished 363 moderate and strong magnetic storms with $Dst \le -50$ nT, for which the following sources were found in the solar wind: the compressed region before high-speed streams (CIRs, 86 magnetic storms); MCs (43 storms); Ejecta (95 storms); all ICME events (MC + Ejecta, 138 storms); Sheath before MCs (Sh_{MC}, 8 storms); Sheath before Ejecta (Sh_E, 56 storms); all Sheaths before MCs and Ejecta ($Sh_{MC} + Sh_E$, 64 storms); and events of an indeterminate type (IND, 75 storms).

For each type of stream, we obtained the regression lines and estimated the correlation coefficients between the |*Dst*| and *AE* indices (the intensities of the ring and auroral currents) and the electric field (E_y).

An analysis of the *Dst* index during the main phases of moderate and strong magnetic storms depending on the solar wind parameters indicated that

(1) A linear relationship (with high correlation coefficients $r_1 > 0.5$) between the |*Dst*| index and the electric field E_y is observed for all eight types of stream;

(2) The |*Dst*| index becomes saturated (i.e., it reaches its maximal value) at large field values ($E_y >$ 11 mV m^{-1}) only for MCs (and possibly for the MC + Ejecta); and

(3) Against a background of the *Dst* index dependence on the E_y field, the value of the *Dst* index is apparently independent of the dynamic pressure *Pd* and the IMF σB fluctuation level.

An analysis of the *AE* index during the main phases of moderate and strong magnetic storms depending on the solar wind parameters indicated the following:

(1) The *AE* index is independent of (or weakly depends on) the electric field value (E_y) for almost all solar wind streams (the correlation coefficient is low, $r < 0.5$) except MCs and Sh_{MC}.

(2) The *AE* index nonlinearly increases with increasing field E_y (the quadratic correlation coefficient is $r_2 = 0.6$) for MC events and linearly increases ($r_1 = 0.76$) for Sh_{MC} events (five events). For MCs, we can assume that the *AE* index linearly increases with increasing field E_y at small its values ($E_y < 11$ mV m^{-1}) but possibly saturates and gradually decreases at strong electric fields ($E_y > 11$ mV m^{-1}). Saturation of *AE* results from the limitation of the polar cap potential owing to the nonlinear nature of the ionosphere–magnetosphere coupling [Weimer et al., 1990].

(3) Against the background of the dependence of the *AE* index on the E_y field, the *AE* index value is independent of (or weakly depends on) the dynamic pressure *Pd* and the IMF σB fluctuation level.

ACKNOWLEDGMENTS

We are pleased that we could use the OMNI database. The OMNI data were obtained from the GSFC/SPDF OMNIWeb site http://omniweb.gsfc.nasa.gov.

This work was supported by the Russian Foundation for Basic Research (project no. 07-02-00042) and by the Department of Physical Sciences, Russian Academy of Sciences (Program 15 Plasma Processes in the Solar System).

REFERENCES

Akasofu, S.-I., Olmsted, N., Smith, E.J., Tsurutani, B., Okida, R., and Baker, D., Solar Wind Variations and Geomagnetic Storms: A Study of Individual Storms Based on High Time Resolution ISEE-3 Data, *J. Geophys. Res.*, 1985, vol. 90A, p. JA090, doi: 10.1029/JA090iA01p00325.

Alves, M.V., Echer, E., and Gonzalez, W.D., Geoeffectiveness of Corotating Interaction Regions as Measured by Dst Index, *J. Geophys. Res.*, 2006, vol. 111, p. A07S05.

Arnoldy, R.L., Signature in the Interplanetary Medium for Substorms, *J. Geophys. Res.*, 1971, vol. 76, no. 22, pp. 5189–5201, doi: 10.1029/JA076i022p05189.

Baker, D.N., Zwickle, R.D., Bame, S.J., Hones, E.W., Tsurutani, B.T., Smith, E.J., and Akasofu, S.-I., An ISEE 3 High Time Resolution Study of Interplanetary Parameter Correlations with Magnetospheric Activity, *J. Geophys. Res.*, 1983, vol. 88A, pp. 6230–6242, doi: 10.1029/JA088iA08p06230.

Borovsky, J.E. and Funsten, H.O., Role of Solar Wind Turbulence in the Coupling of the Solar Wind to the Earth's Magnetosphere, *J. Geophys. Res.*, 2003, vol. 108A, doi: 10.1029/2002JA009601.

Borovsky, J.E. and Denton, M.H., Differences between CME-Driven Storms and CIR-Driven Storms, *J. Geophys. Res.*, 2006, vol. 111, p. A07S08, doi: 10.1029/2005JA011447.

Burton, R.K., McPherron, R.L., and Russell, C.T., An Empirical Relationship between Interplanetary Conditions and Dst, *J. Geophys. Res.*, 1975, vol. 80, pp. 4204–4214.

Cane, H.V., Richardson, I.G., and Cyr, O.C.St., Coronal Mass Ejections, Interplanetary Ejecta and Geomagnetic Storms, *Geophys. Res. Lett.*, 2000, vol. 27, no. 21, pp. 3591–3594.

Davis, T.N. and Sugiura, M., Auroral Electrojet Activity Index AE and Its Universal Time Variations, *J. Geophys. Res.*, 1966, vol. 71, pp. 785–803.

Despirak, I.V., Lubchich, A.A., Yahnin, A.G., Kozelov, B.V., and Biernat, H.K., Development of Substorm Bulges during Different Solar Wind Structures, *Ann. Geophys.*, 2009, vol. 27, pp. 1951–1960.

Dmitriev, A.V., Crosby, N.B., and Chao, J.-K., Interplanetary Sources of Space Weather Disturbances in 1997 to 2000, *Space Weather*, 2005, vol. 3, no. 3, p. 03001, doi:10.1029/2004SW000104.

Echer, E. and Gonzalez, W.D., Geoeffectiveness of Interplanetary Shocks, Magnetic Clouds, Sector Boundary Crossings and Their Combined Occurrence, *Geophys. Res. Lett.*, 2004, vol. 31, no. 9, p. L09808, doi: 10.1029/2003GL019199.

Echer, E., Gonzalez, W.D., and Alves, M.V., On the Geomagnetic Effects of Solar Wind Interplanetary Magnetic Structures, *Space Weather*, 2006, vol. 4, p. S06001, doi: 10.1029/2005SW00200.

Feldstein, Y.I., Modelling of the Magnetic Field of Magnetospheric Ring Current as a Function of Interplanetary Medium Parameters, *Space Sci. Rev.*, 1992, vol. 59, pp. 83–165.

Gonzalez, W.D., Joselyn, J.A., Kamide, Y, Kroehl, H.W., and Rostoker, G., What is a Geomagnetic Storm?, *J. Geophys. Res.*, 1995, vol. 99A, pp. 5771–5792.

Gonzalez, W.D., Tsurutani, B.T., and de Gonzalez, A.L.C., Interplanetary Origin of Geomagnetic Storms, *Space Sci. Rev.*, 1999, vol. 88, pp. 529–562.

Gonzalez, W.D., Clua de Gonzalez, A., Sobral. J., et al., Solar and Interplanetary Causes of Very Intense Geomagnetic Storms, *J. Atmos. Terr. Phys.*, 2001, vol. 63, pp. 403–412.

Gonzalez, W.D., Tsurutani, B.T., Lepping, R.P., and Schwenn, R., Interplanetary Phenomena Associated with Very Intense Geomagnetic Storms, *J. Atmos. Terr. Phys.*, 2002, vol. 64, pp. 173–181.

Gonzalez, W.D. and Echer, E., A Study on the Peak Dst and Peak Negative B_z Relationship during Intense Geomagnetic Storms, *Geophys. Res. Lett.*, 2005, vol. 32, no. 18, p. L18103, doi: 10.1029/2005GL023486.

Huttunen, K.E.J. and Koskinen, H.E.J., Importance of Post-Shock Streams and Sheath Region as Drivers of Intense Magnetospheric Storms and High-Latitude Activity, *Ann. Geophys.*, 2004, vol. 22, pp. 1729–1738.

Huttunen, K.E.J., Koskinen, H.E.J., and Schwenn, R., Variability of Magnetospheric Storms Driven by Different Solar Wind Perturbations, *J. Geophys. Res.*, 2002, vol. 107A, p. JA900171, doi: 10.1029/2001JA900171.

Kane, R.P., How Good Is the Relationship of Solar and Interplanetary Plasma Parameters with Geomagnetic Storms?, *J. Geophys. Res.*, 2005, vol. 110A, p. A02213, doi:10.1029/2004JA010799.

Kershendolts, S.Z., Barkova, E.S., and Plotnikov, I.Ya., Dependence of Geomagnetic Disturbances on Extreme Values of the Solar Wind E_y Component, *Geomagn. Aeron.*, 2007, vol. 47, no. 2, pp. 167–175 [*Geomagn. Aeron.* (Engl. Transl.), 2007, vol. 47, pp. 156–164].

King, J.H. and Papitashvili, N.E., Solar Wind Spatial Scales in and Comparisons of Hourly Wind and ACE Plasma and Magnetic Field Data, *J. Geophys. Res.*, 2004, vol. 110A, p. A02209, doi: 10.1029/2004JA01804.

Lyatsky, W. and Tan, A., Solar Wind Disturbances Responsible for Geomagnetic Storms, *J. Geophys. Res.*, 2003, vol. 108A, p. 2003, doi: 10.1029/2001JA005057.

Maltsev, Y.P., Points of Controversy in the Study of Magnetic Storms, *Space Sci. Rev.*, 2004, vol. 110, no. 3, pp. 227–277.

McPherron, R.L. and O'Brien, T.P., Predicting Geomagnetic Activity: The Dst Index, *Geophys. Monogr. Am. Geophys. Union*, 2001, vol. 155, pp. 339–345.

McPherron, R.L., Kepko, L., and Pulkkinen, T.I., et al., Changes in the Response of the AL Index with Solar cycle and Epoch within a Corotating Interaction Region, *Ann. Geophys.*, 2009, vol. 27, pp. 3165–3178.

Meng, C.I., Tsurutani, D., Kawasaki, K., and Akasofu, S.-I., Cross-Correlation Analysis of the AE Index and the Interplanetary Magnetic Field B_z Component, *J. Geophys. Res.*, 1973, vol. 78, no. 4, pp. 617–629.

O'Brien, T.P. and McPherron, R.L., An Empirical Phase Space Analysis of Ring Current Dynamics: Solar Wind Control of Injection and Decay, *J. Geophys. Res.*, 2000, vol. 105A, pp. 7707–7719.

O'Brien, T.P. and McPherron, R.L., Seasonal and Diurnal Variations of Dst Dynamics, *J. Geophys. Res.*, 2002, vol. 107A, p. JA009435, doi: 10.1029/2002JA009435.

Oh, S.Y. and Yi, Y., Relationships of the Solar Wind Parameters with the Magnetic Storm Magnitude and Their Association with the Interplanetary, *J. Korean Astron. Soc.*, 2004, vol. 37, pp. 151–157.

Plotnikov, I.Ya. and Barkova, E.S., Advances in Space Research Nonlinear Dependence of Dst and AE Indices on the Electric Field of Magnetic Clouds, *Adv. Space Res.*, 2007, vol. 40, pp. 1858–1862.

Richardson, I.G., Cane, H.V., and Cliver, E.W., Sources of Geomagnetic Activity during Nearly Three Solar Cycles (1972–2000), *J. Geophys. Res.*, 2002, vol. 107A, p. JA000504, doi: 10.1029/2001JA000504.

Richardson, I.G., Webb, D.F., Zhang, J., et al., Major Geomagnetic Storms (Dst < –100 nT) Generated by Corotating Interaction Regions, *J. Geophys. Res.*, 2006, vol. 111, p. A07S09, doi: 10.1029/2005JA011476.

Rusanov, A.A. and Petrukovich, A.A., Influence of Solar Wind Parameters on the Level of Geomagnetic Field Fluctuations, *Kosm. Issled.*, 2004, vol. 42, no. 4, pp. 368–375 (Cos. Res. p. 354).

Russell, C.T., McPherron, R.L., and Burton, R.K., On the Cause of Magnetic Storms, *J. Geophys. Res.*, 1974, vol. 79, no. 7, pp. 1105–1109.

Seki, T., Morioka, A., Miyoshi, Y.S., et al., Auroral Kilometric Radiation and Magnetosphere–Ionosphere Coupling Process during Magnetic Storms, *J. Geophys. Res.*, 2005, vol. 110, p. A05206, doi: 10.10292004JA010961.

Siscoe, G.L., Crooker, N.U., and Siebert, K.D., Transpolar Potential Saturation: Roles of Region 1 Current System and Solar Wind Ram Pressure, *J. Geophys. Res.,* 2002a, vol. 107A, p. JA009176., doi: 10.1019/2001JA009176.

Siscoe, G.L., Erickson, G.M., Sonnerup, B.U.O., Maynard, N.C., Schoendorf, J.A., Siebert, K.D., Weimer, D.R., White, W.W., and Wilson, G.R., Hill Model of Transpolar Potential Saturation: Comparisons with MHD Simulations, *J. Geophys. Res.*, 2002b, vol. 107A, p. JA000109, doi: 10.1029/2001JA000109.

Siscoe, G.L., McPherron, R.L., and Jordanova, V.K., Diminished Contribution of Ram Pressure to Dst during Magnetic Storms, *J. Geophys. Res.*, 2005, vol. 110, p. A12227, doi: 10.1029/2005JA011120.

Srivastava, N. and Venkatakrishnan, P., Solar and Interplanetary Sources of Major Geomagnetic Storms during 1996–2002, *J. Geophys. Res.*, 2004, vol. 109A, p. A10103, doi: 10.1029/2003JA010175.

Sugiura, M., Hourly Values of Equatorial Dst for the IGY, *Ann. Int. Geophys. Year*, 1964, vol. 35, pp. 945–948.

Vasyliunas, V.M., Comparative Magnetospheres: Lessons for Earth, *Adv. Space Res.*, 2004, vol. 33, doi: 10.1016/j.asr.2003.04.051.

Vasyliunas, V.M., Reinterpreting the Burton–McPherron–Russell Equation for Predicting Dst, *J. Geophys. Res.*, 2006, vol. 111, p. A07S04, doi: 10.1029/2005HA011440.

Vasyliunas, V.M., The Mechanical Advantage of the Magnetosphere: Solar-Wind-Related Forces in the Magnetosphere–Ionosphere–Earth System, *Ann. Geophys.*, 2007, vol. 25, pp. 255–269.

Vieira, L.E.A., Gonzalez, W.D., Echer, E., and Tsurutani, B.T., Storm-Intensity Criteria for Several Classes of the Driving Interplanetary Structures, *Sol. Phys.*, 2004, vol. 223, no. 1-2, pp. 245–258, doi: 10.1007/s11207-004-1163-2.

Vennerstroem, S., Interplanetary Sources of Magnetic Storms: A Statistical Study, *J. Geophys. Res.*, 2001, vol. 106A, pp. 29175–29184.

Veselovsky, I.S., Panasyuk, M.I., Avdyushin, S.I., et al., Solar and Heliospheric Phenomena in October–November 2003: Causes and Effects, *Kosm. Issled.*, 2004, vol. 42, no. 5, pp. 453–508 (Cos. Res., pp. 435–488).

Vivek Gupta and Badruddin, Interplanetary Structures and Solar wind Behaviour during Major Geomagnetic Perturbations, *J. Atmos. Terr. Phys.*, 2009, vol. 71, pp. 885–896.

Weimer, D.R., Reinleitner, L.A., Kan, J.R., Zhu, L., and Akasofu, S.-I., Saturation of the Auroral Electrojet Current and the Polar Cap Potential, *J. Geophys. Res.*, 1990, vol. 95A, pp. 18981–18987.

White, W.W., Schoendorf, J.A., Siebert, K.D., Maynard, N.C., Weimer, D.R., Wilson, G.L., Sonnerup, B.U.O., Siscoe, G.L., and Erickson, G.M., MHD Simulation of Magnetospheric Transport at the Mesoscale, *Geophys. Monogr. Am. Geophys. Union*, 2001, vol. 125, pp. 229–240.

Wu, C.-C. and Lepping, R.P., Effect of Solar Wind Velocity on Magnetic Cloud-Associated Magnetic Storm Intensity, *J. Geophys. Res.*, 2002, vol. 107A, p. 1346, doi: 10.1029/2002JA009396.

Yermolaev, Yu.I. and Yermolaev, M.Yu., Statistical Relationships between Solar, Interplanetary, and Geomagnetospheric Disturbances, 1976–2000, *Kosm. Issled.*, 2002, vol. 40, no. 1, pp. 3–16 (Cos. Res., pp. 1–4).

Yermolaev, Yu.I., Yermolaev, M.Yu., Zastenker, G.N., Zelenyi, L.M., Petrukovich, A.A., and Sauvaud, J.-A., Statistical Studies of Geomagnetic Storm Dependencies on Solar and Interplanetary Events: A Review, *Planet. Space Sci.*, 2005a, vol. 53, no. 1-3, pp. 189–196.

Yermolaev, Yu.I., Yermolaev, M.Yu., and Nikolaeva, N.S., Comparison of Interplanetary and Magnetospheric Conditions for CIR-Induced and ICME-Induced Magnetic Storms, *EGU Geophys. Res. Abstr.*, 2005b, vol. 7, p. 01064.

Yermolaev, Yu.I., Yermolaev, M.Yu., Lodkina, I.G., and Nikolaeva, N.S., Statistical Investigation of Heliospheric Conditions Resulting in Magnetic Storms, part 1, *Kosm. Issled.*, 2007a, vol. 45, no. 1, pp. 3–11 (Cos. Res., pp. 1–8).

Yermolaev, Yu.I., Yermolaev, M.Yu., Lodkina, I.G., and Nikolaeva, N.S., A Statistical Investigation of Heliospheric Conditions Resulting in Magnetic Storms, part 2, *Kosm. Issled.*, 2007b, vol. 45, no. 6, pp. 489–498 (Cos. Res., pp. 461–470).

Yermolaev, Yu.I. and Yermolaev, M.Yu., Comment on "Interplanetary Origin of Intense Geomagnetic Storms (*Dst* < −100 nT) during Solar Cycle 23" by W.D. Gonzalez et al, *Geophys. Res. Lett.*, 2008, vol. 35, p. L01101, doi: 10.1029/2007GL030281.

Yermolaev, Yu.I., Nikolaeva, N.S., Lodkina, I.G., and Yermolaev, M.Yu., Catalog of Large-Scale Solar Wind Phenomena during 1976–2000, *Kosm. Issled.*, 2009, no. 2, pp. 99–113 (Cos. Res., pp. 81–94).

Yermolaev, Yu.I., Lodkina, I.G., Nikolaeva, N.S., and Yermolaev, M.Yu., Statistical Study of Interplanetary Condition Effect on Geomagnetic Storms, *Kosm. Issled.*, 2010a, vol. 48, no. 6, pp. 461–474 (Cos. Res., pp. 485–500).

Yermolaev, Yu.I., Nikolaeva, N.S., Lodkina, I.G., and Yermolaev, M.Yu., Relative Occurrence Rate and Geoeffectiveness of Large-Scale Types Solar Wind, *Kosm. Issled.*, 2010b, vol. 48, no. 1, pp. 3–32 (Cos. Res., pp. 1–30).

Yurchyshyn, V., Wang, H., and Abramenko, V., Correlation between Speeds of Coronal Mass Ejections and the Intensity of Geomagnetic Storms, *Space Weather*, 2004, vol. 2, p. S02001, doi: 10.1029/2003SW000020.

Zhang, Y., Sun, W., Feng, X.S., Deehr, C.S., Fry, C.D., and Dryer, M., Statistical Analysis of Corotating Interaction Regions and Their Geoeffectiveness during Solar Cycle 23, *J. Geophys. Res.*, 2008, vol. 113, p. A08106, doi: 10.1029/2008JA013095.

Zhu, D., Billings, S.A., Balikhin, M., Wing, S., and Coca, D., Data Derived Continuous Time Model for the *Dst* Dynamics, *Geophys. Res. Lett.*, 2006, vol. 33, p. L04101, doi:10.1029/2005GL025022.